Front. Optoelectron. China 2011, 4(3): 298–307
DOI 10.1007/s12200-011-0139-8

RESEARCH ARTICLE

Impacts of mismatched intrinsic parameter on leader-laggard synchronization between two mutually coupled VCSELs

Lingbo ZENG[1], Tao DENG[1], Zhengmao WU[1], Jiagui WU[1], Guangqiong XIA (✉)[1,2]

1 School of Physics, Southwest University, Chongqing 400715, China
2 State Key Laboratory of Millimeter Waves, Southeast University, Nanjing 210096, China

© Higher Education Press and Springer-Verlag Berlin Heidelberg 2011

Abstract Based on spin-flip model (SFM), the impacts of mismatched intrinsic parameter on leader-laggard chaos synchronization between two mutually coupled vertical-cavity surface-emitting lasers (VCSELs) have been investigated numerically. Results show that, for two VCSELs with identical intrinsic parameter, the switching point of leader-laggard caused by continually varying frequency detuning or injection rate detuning is located at zero frequency detuning or zero injection rate detuning, which indicates that the VCSEL with higher frequency or subject to lower injection level plays a leader role. However, for two VCSELs with mismatched intrinsic parameter, the switched point of leader-laggard will deviate from zero frequency detuning or zero injection rate. Therefore, compared with the results obtained under matched intrinsic parameter, the opposite results have been observed in the range between zero detuning and switching point. Additionally, the offsets of switching point induced by different intrinsic parameters are different, and the influence of line-width enhancement factor is found to be the most significant.

Keywords vertical-cavity surface-emitting laser, mutual coupling, mismatched intrinsic parameter, leader-laggard chaos synchronization

1 Introduction

Vertical-cavity surface-emitting lasers (VCSELs) have been considered as key devices for optical communications, optical interconnection and optical signal processing because of their prominent advantages over traditional edge-emitting lasers, such as low threshold current, single-longitudinal mode, large modulation bandwidth, low cost and wafer-scale integration capability for large arrays configuration [1–6]. Nowadays, mutually coupled VCSELs have attracted considerable interests due to their important application in bidirectional chaos secure communication fields. Since the first demonstration of chaos synchronization between mutually coupled VCSELs [3], nonlinear dynamics, polarization properties and chaos synchronization of mutually coupled scheme have been studied extensively [4–10]. Relevant reports have shown that the chaos synchronization characteristics between two mutually coupled semiconductor lasers (SLs) behave in an unstable way due to stochastic noise, and stochastic leader-laggard synchronization is usually observed in a time dependent manner [11–14]. In order to realize stable chaos synchronization in mutually coupled VCSELs, a method that operation parameters of two VCSELs are asymmetrical has been proposed. For instance, through adjusting frequency detuning between two mutually coupled VCSELs, stable chaos synchronization can be realized [4,15–18]. Additionally, through adopting asymmetrical injection level, stable chaos synchronization can also be obtained and the VCSEL subject to weaker injection rate plays a leader role [4]. However, to our knowledge, all the works mentioned above are focused on the influence of external parameters mismatch on the leader-laggard synchronization between two mutually coupled VCSEL. In practice, there always exist mismatched intrinsic parameters between two VCSELs. Therefore, it is essential to investigate the influences of mismatched intrinsic parameters on the leader-laggard relationship between two mutually coupled VCSEL under asymmetrical external operation parameters. In this paper, based on the spin-flip model (SFM), the impacts of mismatched intrinsic parameter on leader-laggard chaos synchronization

Received March 10, 2011; accepted April 26, 2011

E-mail: gqxia@swu.edu.cn

induced by frequency detuning or injection rate detuning in mutually coupled VCSELs have been investigated numerically, and part results are different from that obtained under the case of two VCSLEs with identical intrinsic parameter.

2 System model

The schematic diagram of two mutually coupled VCSELs system is shown in Fig. 1. The output of VCSEL1 passes through microscopic lens (ML1), and then injects into VCSEL2 after passing through a beam splitter (BS1), an optical isolator (ISO1) and a neutral density filter (NDF1). The output of VCSEL2 experiences a similar process to form mutually delay-coupled structure. The NDF is used to control injected strength. In order to independently control the injection strength of each VCSEL, two separated light paths have been designed in this system. The ISO is used to ensure unidirectional transmission of light.

3 Theory

Based on SFM [1], after considering the effect of external injected field, rate equations for the mutually coupled VCSELs can be described as [6,8]

$$\frac{\mathrm{d}E^x_{1,2}}{\mathrm{d}t} = k(1+\mathrm{i}\alpha)(N_{1,2}E^x_{1,2} - E^x_{1,2} + \mathrm{i}n_{1,2}E^y_{1,2}) - (\gamma_a + \mathrm{i}\gamma_p)E^x_{1,2} + \eta_{21,12}E^x_{2,1}(t-\tau)\exp(-\mathrm{i}\omega_0\tau) + (-1)^{1,2}\mathrm{i}\Delta\omega E^x_{1,2} + F^x_{1,2}, \quad (1)$$

$$\frac{\mathrm{d}E^y_{1,2}}{\mathrm{d}t} = k(1+\mathrm{i}\alpha)(N_{1,2}E^y_{1,2} - E^y_{1,2} - \mathrm{i}n_{1,2}E^x_{1,2}) + (\gamma_a + \mathrm{i}\gamma_p)E^y_{1,2} + \eta_{21,12}E^y_{2,1}(t-\tau)\exp(-\mathrm{i}\omega_0\tau) + (-1)^{1,2}\mathrm{i}\Delta\omega E^y_{1,2} + F^y_{1,2}, \quad (2)$$

$$\frac{\mathrm{d}N_{1,2}}{\mathrm{d}t} = -\gamma_e N_{1,2}\left(1 + \left|E^x_{1,2}\right|^2 + \left|E^y_{1,2}\right|^2\right) + \gamma_e\mu - \mathrm{i}\gamma_e n_{1,2}\left(E^y_{1,2}{E^x_{1,2}}^* - E^x_{1,2}{E^y_{1,2}}^*\right), \quad (3)$$

$$\frac{\mathrm{d}n_{1,2}}{\mathrm{d}t} = -\gamma_s n_{1,2} - \gamma_e n_{1,2}\left(\left|E^x_{1,2}\right|^2 + \left|E^y_{1,2}\right|^2\right) - \mathrm{i}\gamma_e N_{1,2}\left(E^y_{1,2}{E^x_{1,2}}^* - E^x_{1,2}{E^y_{1,2}}^*\right), \quad (4)$$

where subscripts 1 and 2 stand for VCSEL1 and VCSEL2, respectively, and superscripts x and y stand for x and y linear polarization (LP) modes, respectively. E is the slowly varied complex amplitude of the field, N is the total carrier inversion between conduction and valence bands, n accounts for the difference between carrier inversions for spin-up and spin-down radiation channels, k is the decay rate of field, α is line-width enhancement factor, γ_e is the decay rate of total carrier population, γ_s is spin-flip rate, γ_a and γ_p are linear anisotropies representing dichroism and birefringence, respectively, μ is normalized injection current (μ takes the value 1 at threshold), τ is the propagation delay time between the VCSEL1 and VCSEL2, η_{12} (η_{21}) is the injection rate of VCSEL1 (VCSEL2) to VCSEL2 (VCSEL1). In the symmetric reference frame, averaged angle frequency ω_0 and detuning $\Delta\omega$ are defined as follows:

$$\omega_0 = \frac{\omega_1 + \omega_2}{2}, \quad (5)$$

$$\Delta\omega = \frac{\omega_2 - \omega_1}{2}, \quad (6)$$

where ω is free-running optical frequency, and the last terms in Eqs. (1) and (2) represent the spontaneous emission noises which are modeled by Langevin sources [2]:

$$F^x_{1,2} = \sqrt{\beta_{sp}/2}\left(\sqrt{N_{1,2}+n_{1,2}}\xi^1_{1,2} + \sqrt{N_{1,2}-n_{1,2}}\xi^2_{1,2}\right), \quad (7)$$

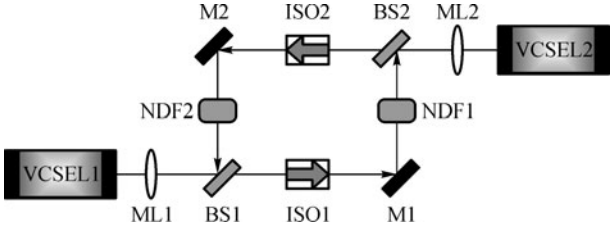

Fig. 1 Schematic diagram of two mutually coupled VCSELs (M: mirror)

$$F_{1,2}^{y} = -\mathrm{i}\sqrt{\beta_{\mathrm{sp}}/2} \times (\sqrt{N_{1,2}+n_{1,2}}\xi_{1,2}^{1} - \sqrt{N_{1,2}-n_{1,2}}\xi_{1,2}^{2}), \quad (8)$$

where ξ_1 and ξ_2 indicate independent Gaussian white noise with zero mean and unitary variance, and β_{sp} is spontaneous-emission rate.

4 Results and discussion

To specifically describe synchronization quality between the two lasers, the quality of chaos synchronization and its time shift can be quantified by calculating shifted correlation coefficient $C(\Delta t)$:

$$C(\Delta t) = \frac{\langle [I_1(t)-\langle I_1\rangle][I_2(t+\Delta t)-\langle I_2\rangle]\rangle}{\{\langle [I_1(t)-\langle I_1\rangle]^2\rangle\langle [I_2(t)-\langle I_2\rangle]^2\rangle\}^{1/2}}, \quad (9)$$

where Δt is the time shift between two VCSELs output, the brackets $\langle\ \rangle$ denote temporal average, $I = |E|^2$ is the output intensity of the laser. A large value of C indicates that good synchronization has been achieved. For perfect chaotic synchronization, C equals to 1.

The rate equations (1)–(4) can be used to solve numerically with the fourth-order Runge-Kutta algorithm. During the calculations, typical parameters are used as follows [2]: $k = 300\ \mathrm{ns}^{-1}$, $\alpha = 3$, $\gamma_{\mathrm{a}} = 0.1\ \mathrm{ns}^{-1}$, $\gamma_{\mathrm{p}} = 10\ \mathrm{ns}^{-1}$, $\gamma_{\mathrm{e}} = 1\ \mathrm{ns}^{-1}$, $\gamma_{\mathrm{s}} = 50\ \mathrm{ns}^{-1}$, $\omega_1 = 2.2176 \times 10^{15}$ rad/s (the corresponding central wavelength is 850 nm), $\mu = 2.5$, $\tau = 3$ ns, $\beta_{\mathrm{sp}} = 10^{-6}\ \mathrm{ns}^{-1}$, and η_{21} fixed at a moderate strength of 30 GHz.

The chaotic time series of each LP of the two VCSELs are given in Figs. 2(a) and 2(b) under the condition of symmetric coupling. Figures 2(c1) and 2(c2) give cross-correlation coefficients corresponding to Figs. 2(a1), 2(b1) and Figs. 2(a2), 2(b2) as a function of time shift. In Figs. 2(c1) and 2(c2), there are two main peaks, respectively, which corresponds to the cross-correlation values shifted by the one-way coupling delay time of $\Delta t = +\tau$ (called C_+) and $\Delta t = -\tau$ (called C_-) [16]. If C_- is smaller than C_+, the chaotic time series of VCSEL1 anticipate that of VCSEL2 by τ. On the contrary, if C_- is larger than C_+, the chaotic time series of VCSEL1 lag behind that of VCSEL2 by τ.

4.1 Effects of frequency detuning or asymmetrical injection level on leader-laggard relationship of two mutually coupled VCSELs with identical intrinsic parameter

The cross-correlation coefficients C_+ and C_- between the two VCSELs are numerically calculated as a function of the frequency detuning under $\Delta\eta = \eta_{21} - \eta_{12} = 0$ GHz in Fig. 3 and the asymmetrical injections under $\Delta\nu = 0$ GHz in Fig. 4. An exchange of the leader-laggard role depends on the sign of the frequency detuning or asymmetrical injection rate, and the switching point of leader-laggard synchronization is exactly at $\Delta\nu = 0$ GHz or $\Delta\eta = 0$ GHz for both x and y LP modes. Therefore, the VCSEL oscillated at higher frequency or subject to weaker injection plays a leader role, which is coincided with the results of Refs. [4,18].

4.2 Effects of mismatched intrinsic parameters on leader-laggard synchronization induced by frequency detuning between two VCSELs

The external parameters such as oscillated frequency and injection strength can be controlled easily, but intrinsic parameters are difficult to be accurately controlled. Therefore, it is essential to investigate the influence of the mismatched parameters on the leader-laggard relationship. For convenience, we fix intrinsic parameters of VCSEL1, and only change the intrinsic parameters of VCSEL2. The relative mismatched intrinsic parameters are defined as

$$\begin{aligned} &\Delta k = (k_2-k_1)/k_1,\ \ \Delta\alpha = (\alpha_2-\alpha_1)/\alpha_1,\\ &\Delta\gamma_{\mathrm{a}} = (\gamma_{\mathrm{a2}}-\gamma_{\mathrm{a1}})/\gamma_{\mathrm{a1}},\ \ \Delta\gamma_{\mathrm{e}} = (\gamma_{\mathrm{e2}}-\gamma_{\mathrm{e1}})/\gamma_{\mathrm{e1}},\\ &\Delta\gamma_{\mathrm{s}} = (\gamma_{s2}-\gamma_{\mathrm{s1}})/\gamma_{\mathrm{s1}}. \end{aligned} \quad (10)$$

Figure 5 shows the dependence of C_+ and C_- on the $\Delta\nu$ when each relative mismatched intrinsic parameter is set at 10%. For the case of $\Delta\nu = 0$ GHz, the leader-laggard relationship is induced only by the mismatched intrinsic parameter. In this case, the VCSEL with smaller k or γ_{e} plays a leader role, while the VCSEL with smaller α, γ_{a} or γ_{s} plays a laggard role. Therefore, after considering the influences of mismatched intrinsic parameters, the location of switching point $\Delta\nu_{\mathrm{sw}}$ is not at $\Delta\nu = 0$ GHz but shifted to negative or positive frequency detuning for different mismatched intrinsic parameter. The location of switching point $\Delta\nu_{\mathrm{sw}}$ shifted to the left (as shown in Figs. 5(a) and 5(d)). That is to say, for $\Delta\nu$ is varied from $\Delta\nu_{\mathrm{sw}}$ to 0 GHz, the VCSEL with lower-frequency will takes the leader role because the influences of mismatched intrinsic parameter plays a dominant role, which is opposite to the result obtained under two VCSELs with matched intrinsic parameter. On the contrary, if the switching point shifted from zero to positive frequency detuning (as shown in Figs. 5(b), 5(c) and 5(e)), for $\Delta\nu$ is varied in the range from zero to $\Delta\nu_{\mathrm{sw}}$, the opposite result can also be obtained after taking the mismatched α, γ_{e} or γ_{s} into account. Figure 6 further shows variation of C_+ and C_- of each LP mode with different internal mismatched parameters (Figs. 6(a) k, 6(b) α, 6(c) γ_{a}, 6(d) γ_{e}, and 6(e) γ_{s}) on condition of $\Delta\nu = 1$ GHz. From this diagram, it can be observed that the curve C_+ and C_- can also appear the cross point. Fortunately, for $\Delta\nu = 1$ GHz, if the mismatched intrinsic parameter is not larger than 10%, the conclusion that the higher-frequency VCSEL takes a leader role is always

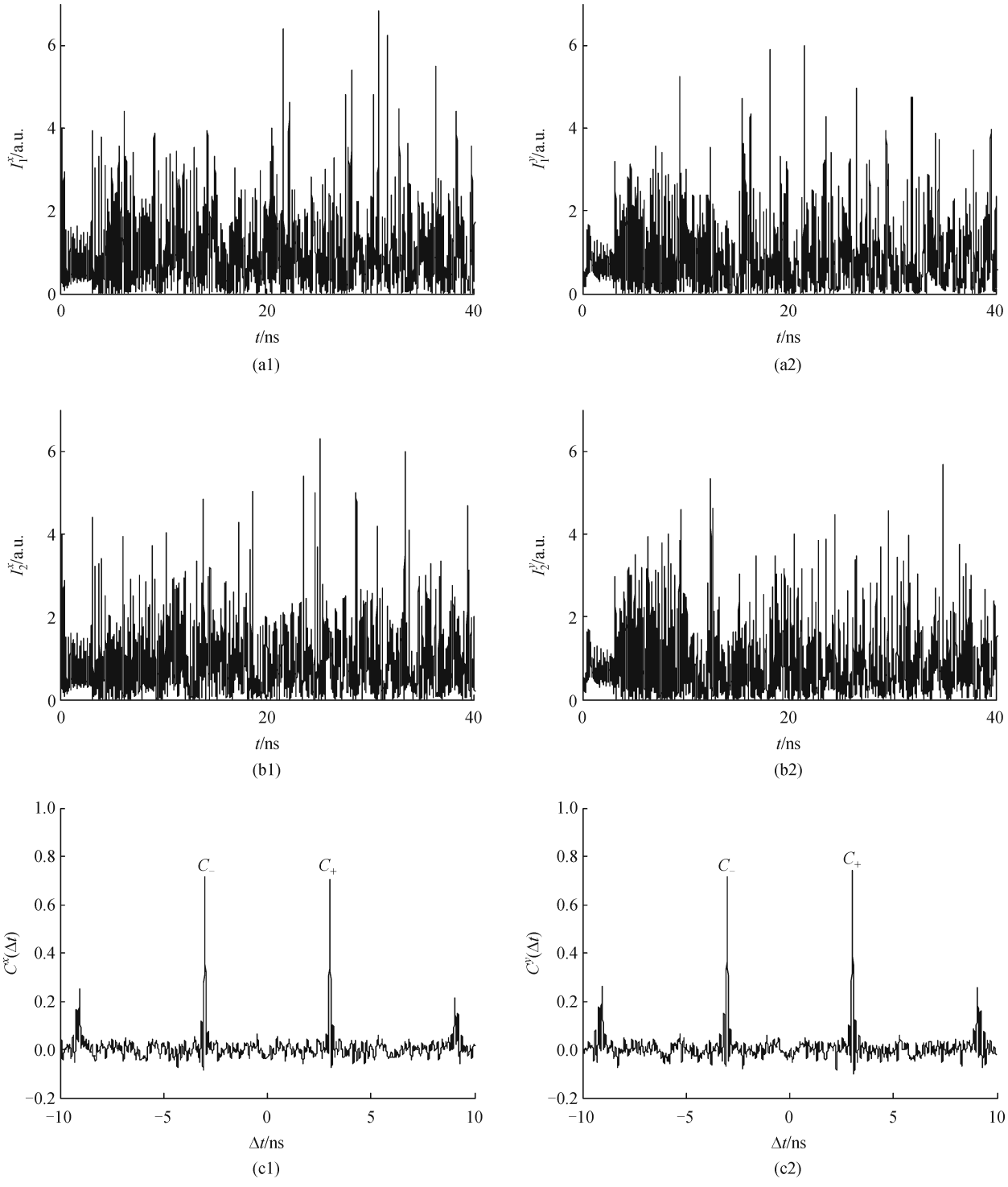

Fig. 2 (a) Time series of x LP, y LP of VCSEL1; (b) time series of x LP, y LP of VCSEL2; (c) corresponding cross-correlation coefficient of x LP, y LP between VCSEL1 and VCSEL2

true. Additionally, it should be pointed out that the mismatched intrinsic parameters may not be only one at most of the time, so the influence of intrinsic parameter mismatch on leader-laggard relationship could be even more complex.

4.3 Effects of mismatched intrinsic parameters on leader-laggard relationship induced by asymmetrical injection strength between two mutually coupled VCSELs

Similar to Fig. 5, Fig. 7 gives the dependence of C_+ and

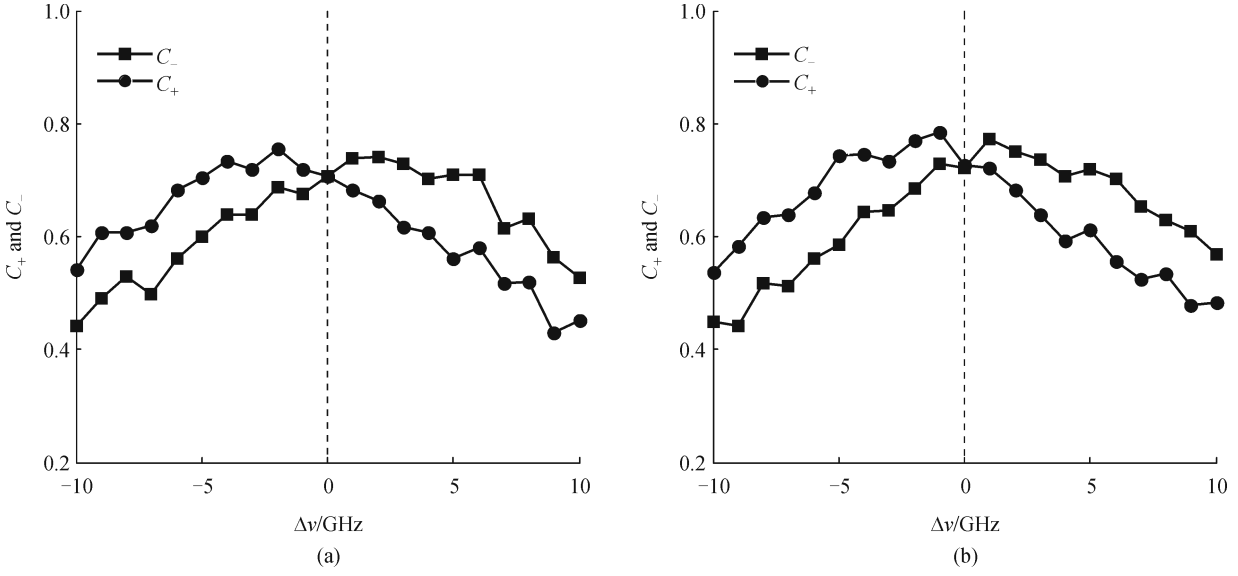

Fig. 3 Dependence of C_+ and C_- on frequency detuning ($\Delta\nu = \nu_2 - \nu_1$). (a) x LP; (b) y LP

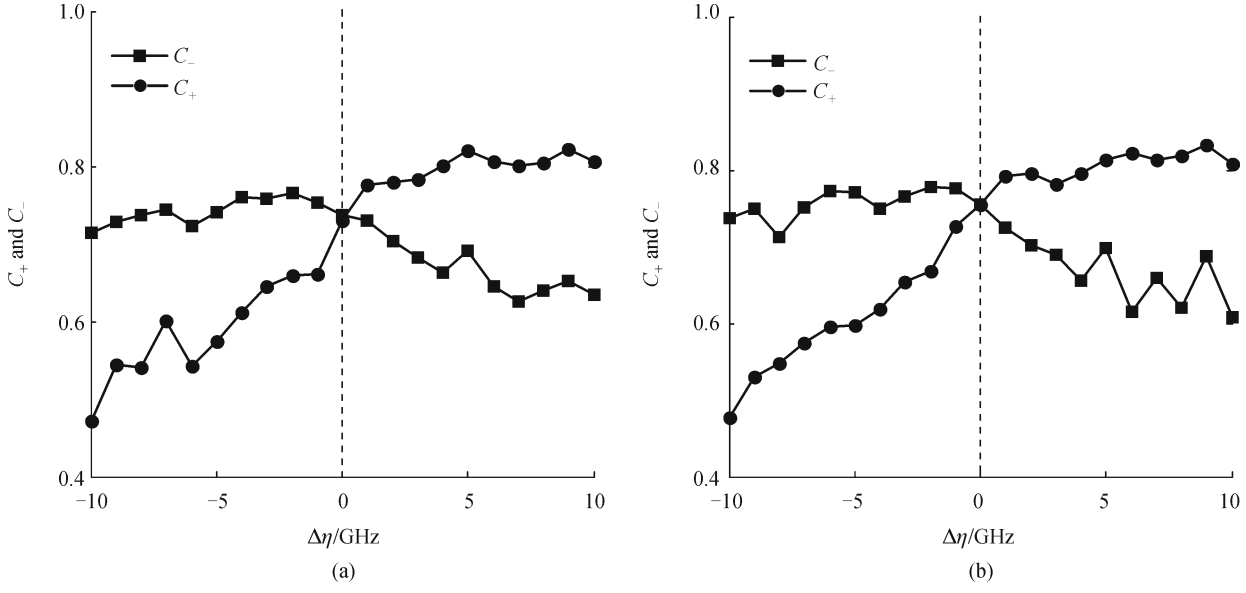

Fig. 4 Dependence of C_+ and C_- on injection detuning ($\Delta\eta = \eta_{21} - \eta_{12}$). (a) x LP; (b) y LP

C_- on $\Delta\eta$ for each of relative mismatched parameters is set at 10%. As seen in Figs. 7(a) and 7(d), the location of switching point $\Delta\eta_{sw}$ slightly shifted to positive value, that is to say, at the range of $0 < \Delta\eta < \Delta\eta_{sw}$, the VCSEL subject to stronger injection level takes the leader role under Δk = 10% or $\Delta\gamma_e$ = 10%. Therefore, combining Fig. 4 and Figs. 7(a) and 7(d), it can be seen that the opposite result has been obtained for $0 < \Delta\eta < \Delta\eta_{sw}$ after considering the mismatched k or γ_e. For mismatched α, γ_a and γ_s, the switching point $\Delta\eta_{sw}$ takes negative value (see Figs. 7(b), 7(c) and 7(e)). So, at the range of $\Delta\eta_{sw} < \Delta\eta < 0$, the VCSEL subject to stronger injection level takes the leader role at this case. Figure 8 shows the dependence of C_+ and C_- on the relative mismatched parameters (Figs. 8(a) k, 8(b) α, 8(c) γ_a, 8(d) γ_e, and 8(e) γ_s) for $\Delta\eta$ fixed at 1.5 GHz. From this diagram, it can be observed that the curve C_+ and C_- can also appear the cross point, but the cross point only appeared when relative mismatch is beyond 10%. It can be predicted that, with the increase of injection level detuning, the separated degree of the two curves C_+ and C_- will enlarge obviously, then the influences of mismatched intrinsic parameters on the relations of anticipating and laggard synchronization will become weak.

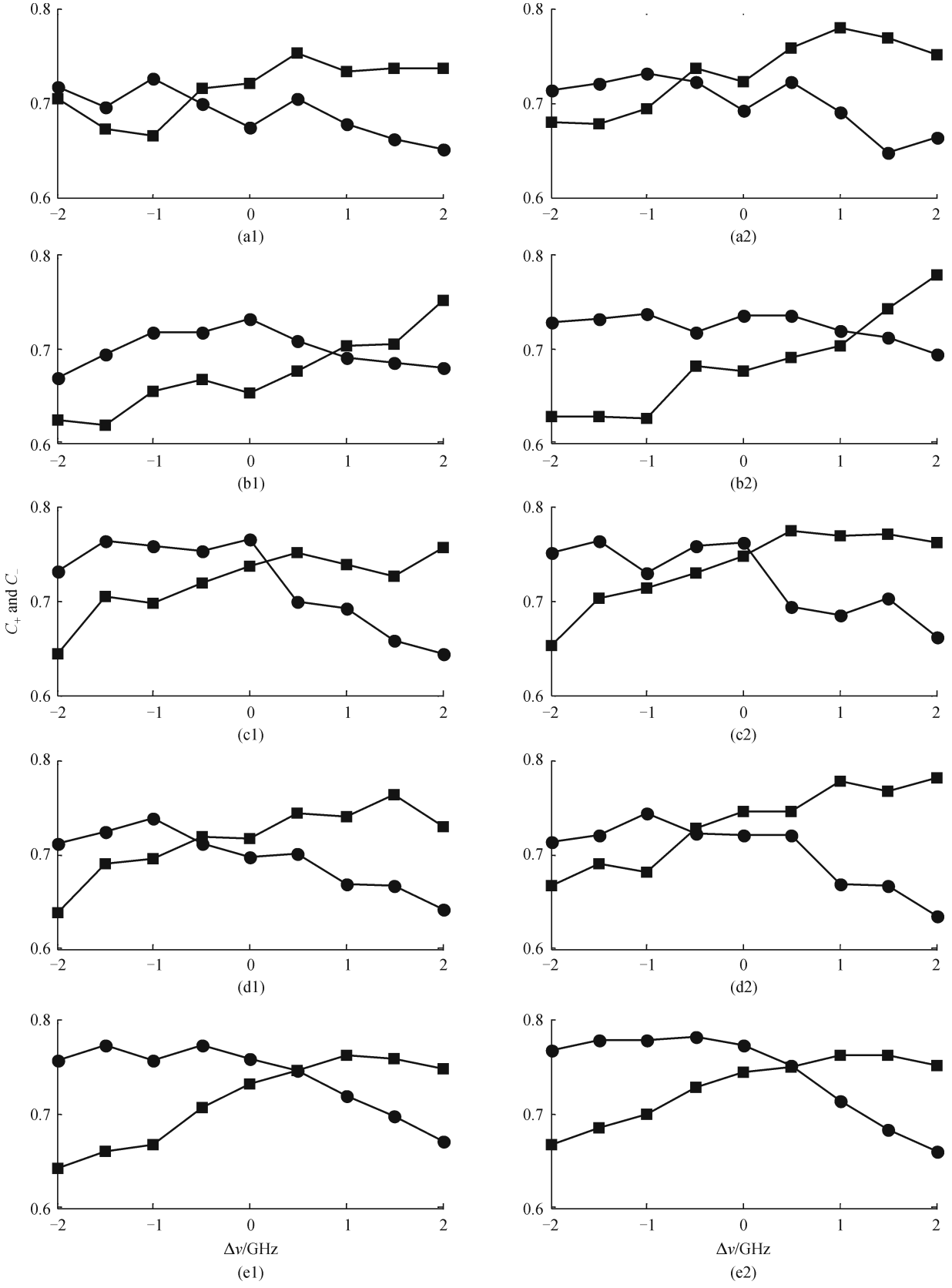

Fig. 5 C_+ (circle) and C_- (square) as a function of frequency detuning for a fixed mismatched (a) k, (b) α, (c) γ_a, (d) γ_e, and (e) γ_s of 10%. Left column is for x LP, and right column is for y LP

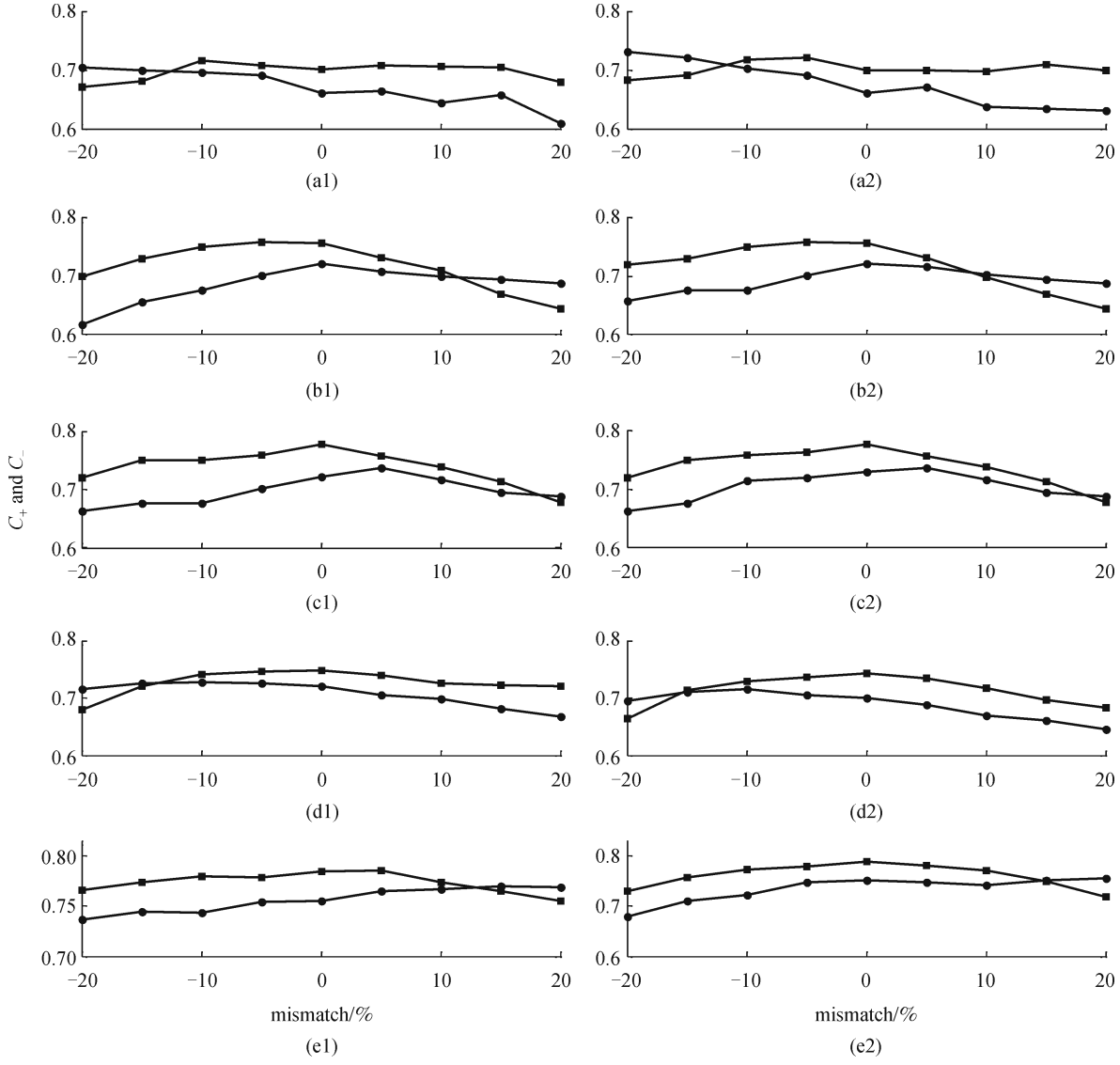

Fig. 6 C_+ (circle) and C_- (square) as a function of mismatched (a) k, (b) α, (c) γ_a, (d) γ_e, and (e) γ_s for a fixed frequency detuning of $\Delta\nu$ = 1 GHz. Left column is for x LP, and right column is for y LP

5 Conclusion

Based on the framework of SFM, the influences of mismatched intrinsic parameter on leader-laggard synchronization induced by frequency detuning or asymmetrical injection between two VCSELs are investigated numerically. The results show that, for the case of frequency detuning, the switching point appeared at zero detuning when the intrinsic parameters of two VCSELs are identical. Therefore, the VCSEL oscillated at higher frequency takes the leader role. However, after taking the mismatched intrinsic parameter into account, the switching point will deviate from zero frequency detuning. Therefore, between the switch point and the zero frequency detuning, the result that VCSEL is leader is opposite to that obtained under identical intrinsic parameters between two VCSELs. For the case of asymmetrical injection, the transition point appeared at zero detuning of injection strength when internal parameters of two VCSELs are identical, and the VCSEL subject to lower-injection plays a leader role. However, the switching point slightly shifted to positive value for mismatched k or γ_e, while the switching point slightly shifted to negative value for mismatched α, γ_a or γ_s. In general, after considering the influences of mismatched intrinsic parameter, the switching point of leader-laggard synchronization will deviate from the zero frequency detuning or symmetric injection level as observed experimentally in Ref. [16]. Additionally, all of the results for x LP mode are as the same as those for y LP mode.

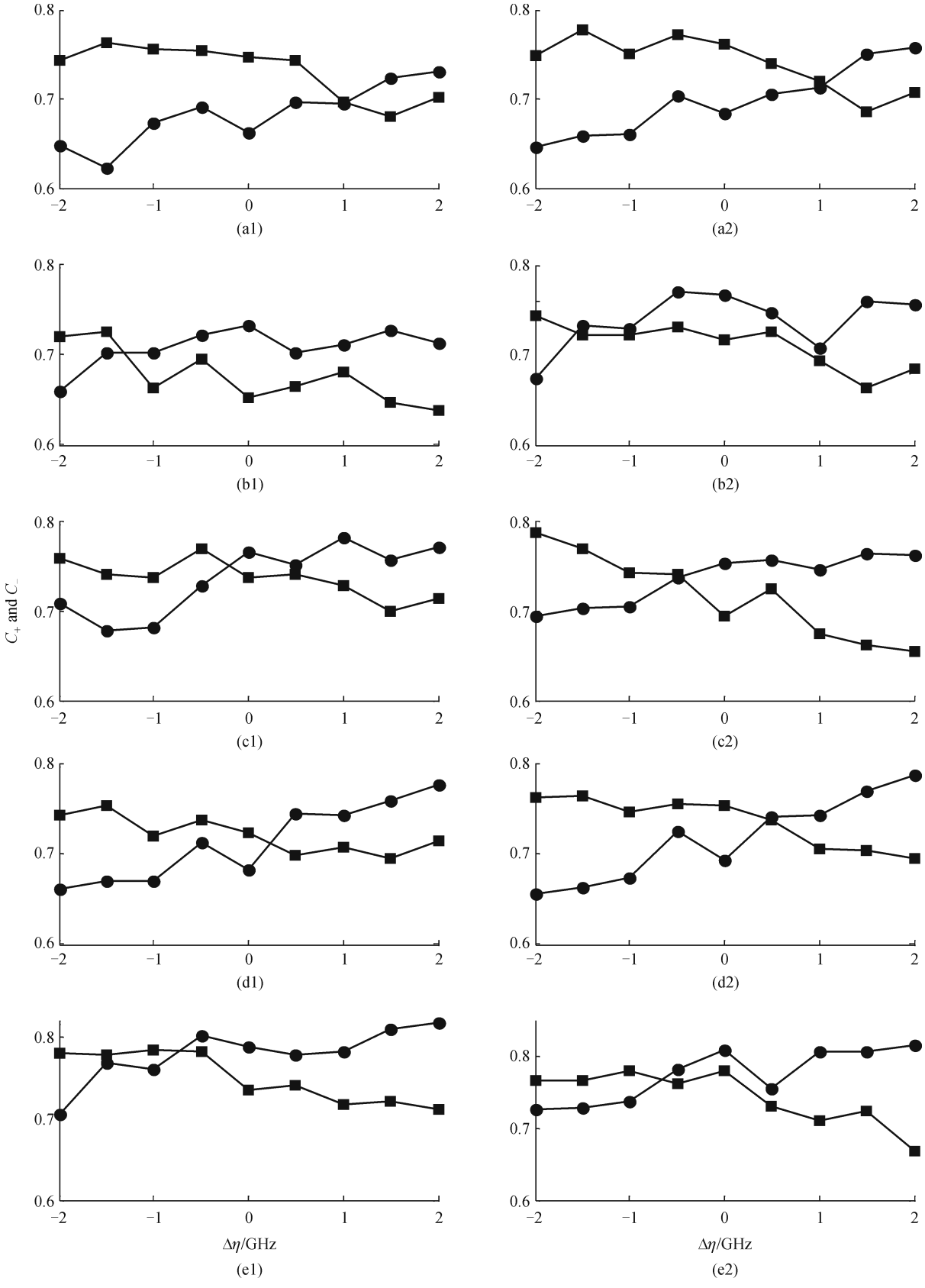

Fig. 7 C_+ (circle) and C_- (square) as a function of the detuning of injection strength for a fixed mismatched (a) k, (b) α, (c) γ_a, (d) γ_e, and (e) γ_s of 10%. Left column is for x LP, and right column is for y LP

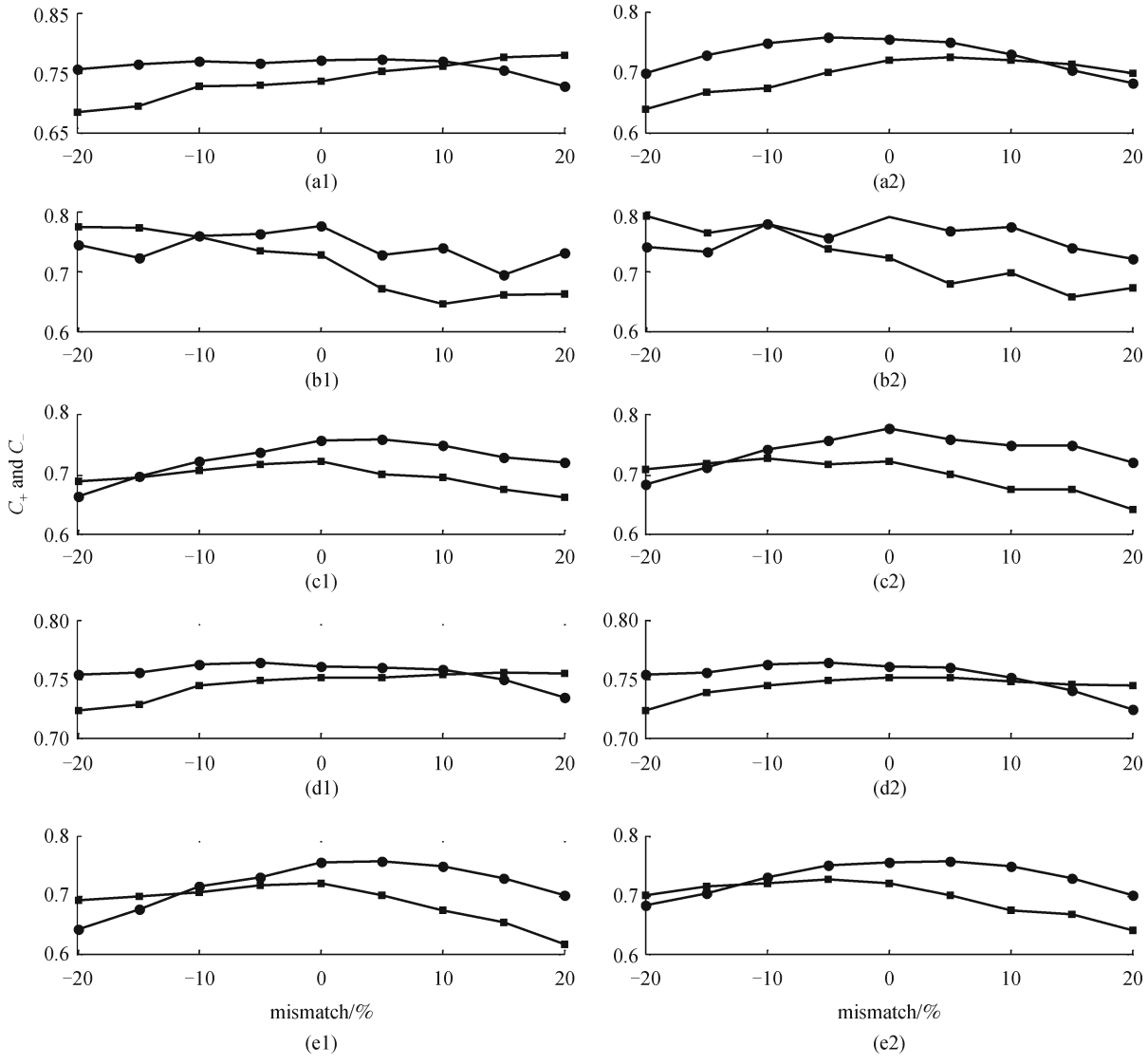

Fig. 8 C_+ (circle) and C_- (square) as a function of mismatched (a) k, (b) α, (c) γ_a, (d) γ_e, and (e) γ_s for a fixed detuning of injection strength of $\Delta\eta$ = 1.5 GHz. Left column is for x LP, and right column is for y LP

Acknowledgements This work was supported by the National Natural Science Foundation of China (Grant Nos. 11004161, 61078003 and 60978003), the Natural Science Foundation of Chongqing City (No. 2010BB9125), the Fundamental Research Funds for the Central Universities (No. XDJK2010C021), and the Open Fund of the State Key Lab of Millimeter Waves (No. K201109).

References

1. Regalado J M, Prati F, Miguel M S, Abraham N B. Polarization properties of vertical-cavity surface-emitting lasers. IEEE Journal of Quantum Electronics, 1997, 33(5): 765–783
2. Liu J, Wu Z M, Xia G Q. Dual-channel chaos communication in unidirectional coupled VCSELs with polarization-rotated optical feedback and polarization-rotated optical injection. Optics Express, 2009, 17(15): 12619–12626
3. Fujiwara N, Takiguchi Y, Ohtsubo J. Observation of the synchronization of chaos in mutually injected vertical-cavity surface-emitting semiconductor lasers. Optics Letters, 2003, 28 (18): 1677–1679
4. Zhang W L, Pan W, Luo B, Li X F, Zou X H, Wang M Y. Polarization-resolved dynamics of asymmetrically coupled vertical-cavity surface-emitting lasers. Journal of the Optical Society of America. B, Optical Physics, 2008, 25(2): 153–158
5. Zhang W L, Pan W, Luo B, Li X F, Zou X H, Wang M Y. Polarization switching of mutually coupled vertical-cavity surface-emitting lasers. Journal of the Optical Society of America. B, Optical Physics, 2007, 24(6): 1276–1282
6. Vicente R, Mulet J, Mirasso C R, Sciamanna M. Bistable polarization switching in mutually coupled vertical-cavity surface-emitting lasers. Optics Letters, 2006, 31(7): 996–998
7. Zhang W L, Pan W, Luo B, Li X F, Zou X H, Wang M Y. Polarization switching and synchronization of mutually coupled

vertical-cavity surface-emitting semiconductor lasers. Chinese Physics, 2007, 16(7): 1996–2002

8. Vicentea R, Mirasso C R. Dynamics of mutually coupled VCSEL's. Proceedings of SPIE, 2004, 5349: 331–338
9. Erzgräber H, Lenstra D, Krauskopf B, Fischer I. Dynamical properties of mutually delayed coupled semiconductor lasers. Proceedings of SPIE, 2004, 5452: 352–361
10. Vicentea R, Muleta J, Sciamannab M, Mirasso C R. Simple interpretation of the dynamics of mutually coupled semiconductor lasers with detuning. Proceedings of SPIE, 2004, 5349: 307–318
11. Heil T, Fischer I, Elsässer W, Mulet J, Mirasso C R. Chaos synchronization and spontaneous symmetry-breaking in symmetrically delay-coupled semiconductor lasers. Physical Review Letters, 2001, 86(5): 795–798
12. Rogister F, García-Ojalvo J. Symmetry breaking and high-frequency periodic oscillations in mutually coupled laser diodes. Optics Letters, 2003, 28(14): 1176–1178
13. Shen J T, Fan C R, Wu J G, Xia G Q, Ding L, Li N Y, Wu Z M. Conversion between anticipating and lag chaos synchronization induced by different bias current levels in mutually delay-coupled semiconductor lasers. Applied Physics B: Lasers and Optics, 2011, 103(4): 941–945
14. González C M, Torrent M C, García-Ojalvo J. Controlling the leader-laggard dynamics in delay-synchronized lasers. Chaos, 2007, 17(3): 033122
15. Panajotov K, Uchida A, Sciamanna M. Synchronization of chaos in mutually coupled VCSELs: numerical study. In: CLEOE and IQEC 2007 Conference Digest. 2007, JSI_5:1-1
16. Ozaki M, Someya H, Mihara T, Uchida A, Yoshimori S, Panajotov K, Sciamanna M. Leader-laggard relationship of chaos synchronization in mutually coupled vertical-cavity surface-emitting lasers with time delay. Physical Review E, 2009, 79(2): 026210
17. Uchida A, Someya H, Ozaki M, Tanaka K, Yoshimori S, Panajotov K, Sciamanna M. Synchronization of chaos in mutually coupled vertical-cavity surface-emitting lasers with time delay. In: Proceedings of IEEE/LEOS Winter Topicals Meeting Series on Nonlinear Dynamics in Photonic System. 2009, 126–127
18. Panajotov K, Sciamanna M, Thienpont H, Uchida A. Impact of light polarization on chaos synchronization of mutually coupled VCSELs. Optics Letters, 2008, 33(24): 3031–3033